J Clin Periodontol 2007; 34: 618–624 doi: 10.1111/j.1600-051X.2007.01082.x

Journal of Clinical Periodontology

Effect of constant strain rate, composed of varying amplitude and frequency, of early loading on peri-implant bone (re)modelling

E. De Smet[1], S. V. N. Jaecques[2], J. J. Jansen[3], F. Walboomers[3], J. Vander Sloten[2] and I. E. Naert[1]

[1]Department of Prosthetic Dentistry/BIOMAT Research Group, School of Dentistry, Oral Pathology and Maxillofacial Surgery, K. U. Leuven, Kapucijnenvoer, Leuven, Belgium; [2]Department of Mechanical Engineering, Division of Biomechanics and Engineering Design, K. U. Leuven, Celestijnenlaan, Leuven, Belgium; [3]Department of Biomaterials/Dentistry, University Medical Center, University of Nijmegen, Nijmegen, The Netherlands

De Smet E, Jaecques SVN, Jansen JJ, Walboomers F, Vander Sloten J, Naert IE. Effect of constant strain rate, composed by varying amplitude and frequency, of early loading on peri-implant bone (re)modelling. J Clin Periodontol 2007; 34: 618–624. doi: 10.1111/j.1600-051X.2007.01082.x.

Abstract

Aim: Examine the effect of varying components of strain rate – amplitude *versus* frequency – while maintaining a constant strain rate of early controlled mechanical loading on implant stability, peri-implant bone mass and bone-to-implant contact.

Material and Methods: Three groups of guinea-pigs received TiO_2-blasted implants in both tibiae. One week after installation test implants were loaded 5 days/week during 4 weeks. The contra-lateral implants were the unloaded controls. Strain rate was kept constant (1600 $\mu\varepsilon$/s), while amplitude and frequency were varied per group. Implant stability was followed by resonance frequency analysis. Animals were sacrificed, and ground sections were prepared to rate bone-to-implant contact and bone mass.

Results: All implants ($n = 78$) integrated uneventfully. A significant positive effect ($p = 0.03$) of early loading on bone mass was observed in the distal medullar cavity. A significant difference in bone mass between test and control implants was evidenced between the groups ($p = 0.03$ and 0.04). A significant increase in implant stability and bone-to-implant contact could not be shown.

Conclusions: Early controlled stimulation of peri-implant bone is related to amplitude/frequency and not to strain rate as such, considering a constant stimulation time. An increase of bone mass around early-loaded implants was shown. This cortical bone model is most sensitive to low-frequency/high-amplitude stimulation.

Key words: animal study; early loading; frequency; guinea-pig; implant; strain; strain rate

Accepted for publication 18 February 2007

Currently in the clinic, there is a shift towards faster implant loading. This results in a decrease in discomfort for the patients compared with the long healing times in the delayed loading protocol. The local mechanical loading situation is believed to be a strong determinant in the processes of tissue differentiation and bone formation/resorption around implants. Early/immediate loading might offer the potential to stimulate osteogenic effects during implant healing under specific conditions. The present work is part of a larger European Community – project to analyse adaptive bone (re)modelling around implants that receive controlled mechanical stimulation early post-operatively. The aim of this overall project (http://imload.mech.kuleuven.ac.be) is to develop a model of tissue differentiation that may predict the in vivo bone response on specific mechanical parameters. With such a model, mechanical stimulation parameters that accelerate or consolidate osseointegration in cases of early and immediate loading can be selected or the design of the implants can be optimized as a function of early and immediate loading.

Important parameters for osteogenic (bone forming) mechanical stimulation can be identified from the literature (e.g. strain rate, peak strain, frequency, number of cycles/duration) (Turner 1998). In earlier guinea-pig experiments on early controlled mechanical loading (De Smet et al. 2006), six groups with varying strain rates were compared. A significant positive effect of stimulation on

Conflict of interests and source of funding statement

The authors declare that they have no conflict of interest.

This research was funded by the European Community: IMLOAD QLK6-CT-2002-02442.

peri-implant bone mass (BM) could be shown. However, the effect increased with decreasing strain rate of early loading, reaching an optimal osteogenic stimulus at a strain rate of 1600 $\mu\varepsilon$/s in the cortical bone at a distance of 1.3 mm from the implant surface. An increase in peri-implant BM could be shown with increasing force amplitude. Considering stimulation frequency results were in favour of a low-frequency stimulation of 3 Hz. In these experiments, the number of cycles was kept constant, resulting in variable stimulation times. For the high-frequency stimulation groups, test implants were only loaded 1 min./day, which could explain the lower osteogenic effect. The benefit of high-frequency stimulation could be that lower force amplitudes had to be applied, which were less manipulative, while resulting in a higher strain rate stimulation.

The hypothesis of the present study was that well-controlled implant loading does lead to an improved bone-healing response, considering more and accelerated peri-implant bone formation, resulting in an accelerated increase in implant stability.

The a priori goal of this guinea-pig study was to identify the effect of early load strain rate (= frequency × strain) *versus* strain/frequency of a sinusoidal varying load. The strain rate was kept constant for the three groups, while the amplitude and frequency were varied in an inversely proportional manner. If strain rate is the determining factor of early controlled mechanical loading, no difference in implant stability, peri-implant BM and bone-to-implant contact should be expected between the three groups.

Material and Methods

Surgical procedure

Three series of male, skeletally mature guinea-pigs ($n = 13$ on average per series) received one percutaneous customized Ti implant (Astra Tech, Mölndal, Sweden) in the distal part of both tibiae. Surgery was performed under general injection anaesthesia [Ketamine Ceva 1000® (Ceva Animal Care, Brussels, Belgium) 50 mg/kg i.m. and Xyl-M® (V. D. K., Arendonk, Belgium) 2% sol. 0.25 ml/kg i.m.]. A longitudinal incision was made on the medial side of the tibia just above the ankle joint. Both cortices of the tibia were perforated with low rotational speed under continuous external saline cooling to a diameter slightly smaller (0.3 mm) than the implant's diameter to obtain a good primary stability of the implants. Implants were inserted by manual torque. Resorbable sutures (Vicryl® 3–0, Ethicon GmbH, Norderstadt, Germany) were used to close the longitudinal incisions (investigator E. D.). Post-operatively, the guinea-pigs received doxycycline (Vibravet®, Pfizer, Belgium) (0.5 mg/kg p.o.) for 5 days to prevent infection. Additionally, strict cage hygiene was maintained by changing the bedding material daily during the study period. Buprenorfin (Temgesic®, Reckit & Coleman, UK) (0.05 mg/kg s.c.) was used as analgesia.

Implants

Customized screw-shaped TiO_2-blasted (Ra: 1.74 m) Ti6Al4V implants (1.8 × 5 mm) (Astra Tech) were used (Fig. 1). The percutaneous part was conically shaped and allowed a tight connection of the Osstell transducer and stimulation device by screw tightening.

Mechanical stimulation

Skin healing was allowed for 1 week after implant installation. Implants were allocated at random in the right or left tibia of the guinea-pig as a test or control implant. The control implants were unloaded, while the test implants received a sinusoidal varying bending moment with a force-controlled electromechanical shaker (Model 4810, Brüel and Kjaer, Naerum, Denmark). All test implants of the three groups received a constant stimulation period of 10 min./day, 5 days/week, for four successive weeks. The strain rate of the mechanical stimulation was set at 1600 $\mu\varepsilon$/s as an optimum from earlier results (De Smet et al. 2006) for all three groups, while force amplitude and stimulation frequency were varied in an inversely proportional manner. The number of cycles was adjusted so that the stimulation time was kept constant for 10 min. in all three series, with a minimum of 1.800 cycles (Kaspar et al. 2002). The strain rates listed in Table 1 were calculated from cadaver strain gauge measurements, with the strain gauge glued on the outer surface of the tibial bone in the direction of the stimulation lever arm, at a 1.3 mm distance from the implant surface (Fig. 2a–c). During stimulation, the animals were under full inhalation anaesthesia (Fluothane®, halothane, Zeneca, Belgium/Forene®, isoflurane, Abbott, UK) and the hind leg was firmly fixed to ensure reproducible mechanical stimulation. The horizontal lever was attached onto the implant, in alignment with the long axis of the tibia. Thus, the forces acted parallel to the long axis of the implants. At a distance of 20 mm distally from attachment point, the electromechanical shaker applied the sinusoidally varying force through a piezo load cell (model PCB 208B03, PCB Piezotronics, Depew NY, USA). Force was transferred from the load cell to the lever through an adjustable pin. A preload of approximately 1 N ensured continuous contact with the lever. Signals from the load cell were amplified by a PCB 480D06 amplifier (10 s time constant) (PCB Piezotronics) and captured by a Keithley 1702AO 12 A/D data acquisition card (Keithley Instruments B.V., Sint-Pieters-Leeuw, Belgium). The same card was also used to send the

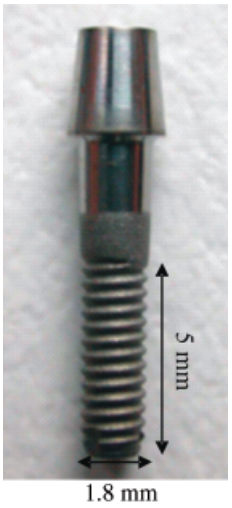

Fig. 1. Customized Ti6Al4V implants (1.8 × 5 mm) (Astra Tech) TiO_2-blasted resulting in an Ra value of 1.74 μm.

Table 1. Mechanical loading parameters of the early stimulation experiment of screw-shaped TiO_2-blasted Ti6AL4V implants in the distal tibia of the guinea-pig model

Group	Cycle no. (n)	Force amplitude (N)	Strain amplitude ($\mu\varepsilon$)	Frequency (Hz)	Strain rate ($\mu\varepsilon$/s)
1 ($n = 10$)	1800	2	533	3	1600
2 ($n = 14$)	6000	0.6	160	10	1600
3 ($n = 15$)	18000	0.2	53	30	1600

n, number of guinea-pigs.

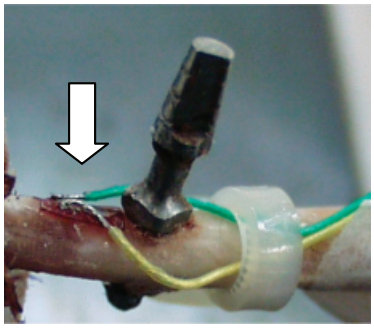

a

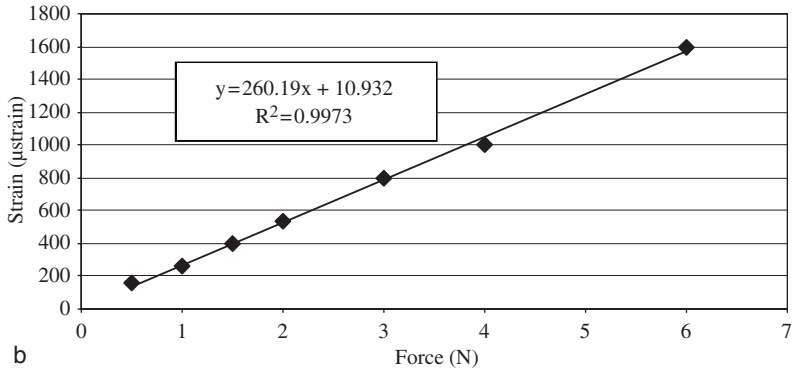

b

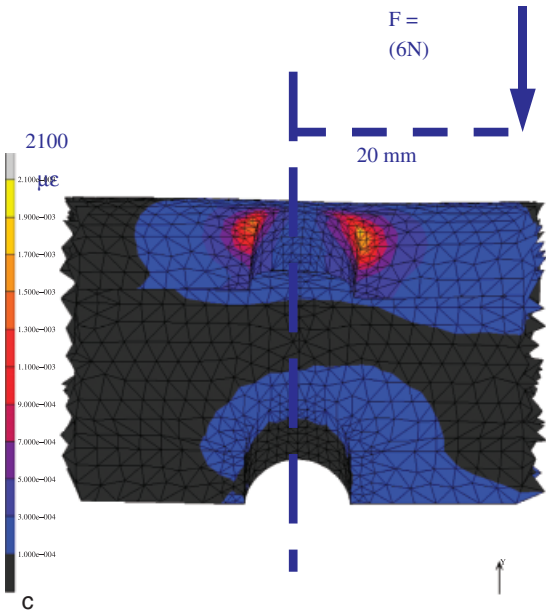

c

Fig. 2. (a) Strain gauge (white arrow) attached to guinea-pig tibia at a distance of 1.3 mm from the implant (cadaver calibration experiment). (b) Measured strain as a function of the amplitude of the force applied by the mechanical stimulator on the 20 mm long lever. The strains increase linearly with the force amplitude. This ex vivo calibration experiment was performed three times on one dissected guinea-pig tibia. (c) Simplified finite element model of part of a guinea-pig tibia with a cylindrical implant showing bone strains of 2000–3000 $\mu\varepsilon$ (yellow) in the cortical bone in the immediate vicinity of the implant for a force of 6 N applied on a lever of 20 mm attached on the implant.

control signal for the shaker through a DC-coupled power amplifier (custom made). Control software, including a force-controlled feedback loop, data acquisition and data visualization, was implemented as a TestPoint application on a Pentium-100 PC (Dell, Bracknell, UK) running under MS Windows 95. Normal cage activity was allowed between the loading sessions (investigators E. D. and S. J.)

Stability measurements

To rate the stability of the implant fixation, the principle of vibration analysis, as commercially available through the Osstell® device (Integration Diagnostics, Savedalen, Sweden), was used. A customized transducer was manufactured by the latter to fit the percutaneous part of the implant. For group 1, implant stability measurements were performed at implant installation, 1 week after and from then on every 2 weeks, for test as well as for control implants. For the other groups 2 and 3, the protocol was adjusted to follow the implant stability weekly (investigator E. D.)

The protocols for all guinea-pig experiments were approved by the ethical committee of the Animal Research Facility of the KULeuven.

Specimen preparation

At the end of the fourth week of mechanical stimulation, animals were sacrificed. Post-mortem bone segments were fixed in 10% buffered formalin solution. Subsequently, serial ground sections were prepared (Van Der Lubbe et al. 1988, Klein et al. 1994). The sections ($n = 3$ per implant) were cut in the loading direction parallel to the long axis of the tibia and the implant. The sections were stained with methylene blue and basic fuchsin for histology and morphometric analysis.

Histological analysis

A light microscope (Leica Microsystems GmbH, Wetzlar, Germany) was used for the histological evaluation dealing with a general description of the tissues surrounding the implants.

Histomorphometrical analysis

The histomorphometrical analysis was carried out by means of a light microscope (Microsystems GmbH) connected to a PC, equipped with a video and image analysis system (Leica Q-win® Pro-image analysis system, Wetzlar, Germany). Digital images were made of the proximal and distal half of the histological section. A routine was written in the program for standardized segmentation of the bone on the digital images of the histological sections. Determination of the regions of interest allowed manual adjustments. All quantitative measurements were based on the average of three sections per implant. The following histomorphometrical analyses were carried out:

1. Total bone contact (TBC) (%) = [total length of bone contact (μm)/total length of implant surface (μm)] × 100, along the proximal and distal implant surfaces.
2. BM (%) = [area of bone in the reference area (μm^2)/reference area (μm^2)] × 100.

Based on the BM, the difference in BM (δ BM) between test and control side was calculated. Quantification of BM (%) was performed for both the upper and lower cortices and the medullar cavity at 500, 1000 and 1500 μm from the proximal and distal implant surfaces (Fig. 3) (investigator E. D.).

Statistical analysis

The histomorphometrical data were analysed by fitting a linear mixed model with an appropriate variance – co-variance matrix to account for the correlation between measurements on the same guinea-pig (test/control). The model included group, stimulation and their interaction as fixed effects. A Tukey test adjusted for multiple testing at $\alpha = 0.05$.

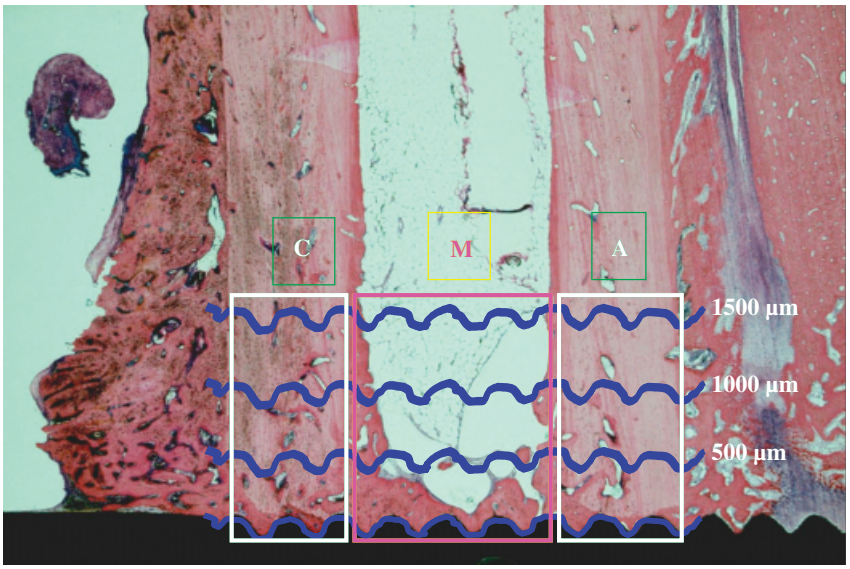

Fig. 3. Quantification of bone mass (%) was performed on digital images of the proximal and distal half of the histological slices, at 3 × 3 regions of interest (ROI): at 500, 1000 and 1500 μm from the proximal and distal implant surfaces for the cervical cortex (C500, C1000, C1500), the medullar cavity (M500, M1000, M1500) and for the apical cortex (A500, A1000, A1500).

Results

Animal and implant outcome

All animals survived well during the course of the experiment. Owing to the 1-week-healing period of the skin, preceding the implant stimulation regimen, the skin remained healthy during the whole course of the experiment. All, test and control implants ($n = 78$), integrated uneventfully. At sacrifice, no clinical mobility of any of the implants could be evidenced.

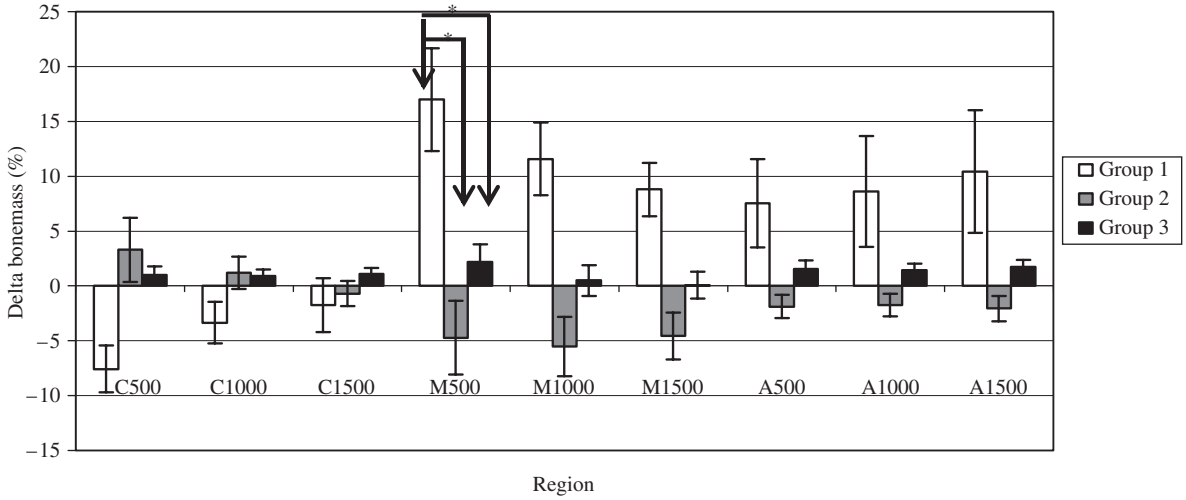

Fig. 4. Mean bone mass (BM) (%) quantification was performed for both the upper (C) and lower (A) cortices and the medullar (M) cavity 500, 1000 and 1500 μm from the proximal and distal implant surfaces. Based on the BM, the difference in BM between the test and control sides [δ BM (%) = BM at the stimulated minus BM at the control side] was calculated for the three groups and presented here for all regions at the distal and proximal sides. A significant difference in δ BM between Groups 1 and 2 ($p = 0.03$)/Group 3 ($p = 0.04$) for the M500 region was evidenced. For the M1000 and M1500 region, nor for the cortical (cervical and apical) regions of interest, a statistically significant difference in δ BM between the groups was shown.

Table 2. Mean bone-to-implant contant (%) (SEM) of test and control implants, for the distal and proximal surface, for the three guinea-pig series

Group	Test		Control	
	distal	proximal	distal	proximal
1 ($n = 10$)	78.6 (1.9)	65.34 (1.7)	76.65 (3.0)	65.32 (3.0)
2 ($n = 14$)	87.7 (3.0)	84.01 (2.4)	79.03 (2.9)	77.83 (2.8)
3 ($n = 15$)	79.2 (2.9)	67.7 (2.0)	65.17 (1.6)	69.71 (2.5)

n, number of guinea-pigs.

Bone mass

On the histological slices, new bone is formed along the implant surface in the medullar cavity. Not only along the implant surface but also along the endosteum away from the implant new bone is formed in the medullar cavity. The area of new bone formed from the cervical endosteum is systematically larger than along the apical endosteum. Systematically more re-modelled bone could be seen at the cervical than at the apical cortex, both for test and control implants.

Histomorphometry showed a significant effect of stimulation on BM ($p = 0.03$) at the distal side of the implants. A significant difference in δ BM between groups 1 and 2 ($p = 0.03$)/ group 3 ($p = 0.04$) for the M500 region was evidenced. No effect of stimulation and of group could be shown for the regions M1000 and M1500 (Fig. 4).

Bone contact

The average percentages (SEM) of bone-to-implant contact along the proximal and distal surfaces of test and control implants ranged between 65.3 (1.68) and 87.70 (3.01) (Table 2). Despite a tendency, there was neither a significant difference in total bone-to-implant contact between the compression (distal) and the tensile (proximal) sides, nor between the test and control implants, or among the different series.

Implant stability

Initial implant stability ranged between a mean peak resonance frequency of 5.100 and 5.500 Hz depending on the groups (Fig. 5a–c). Statistically significant differences were neither found between the test and control implants nor between the groups, or over time.

Discussion

To explain bone adaptation to mechanical loading, Frost's mechanostat (Frost 1987) focused on bone strain amplitude. He described a window of mechanical usage, which is defined by an upper boundary (1500 μstrain), called the minimum effective strain above which bone undergoes modelling and changes its structure in order to reduce the local stress and strain (Frost 1983). It had been shown that above a certain strain threshold, bone formation is initiated in cortical bone (Rubin & Lanyon 1985, Turner et al. 1994) and that with increasing strain, bone responds with increasing formation activity (Hsieh et al. 2001). Excessive load has been studied and even the borderline of the bone-implant failure value has been quantified in the rabbit model (Duyck et al. 2001). The strain estimated from CT-based finite element models associated with overload induced resorption was 4200 μstrain/s. Frost (1992) considered 4000 μstrain a possible threshold for pathological bone overload, suggesting that higher strains would lead to the accumulation of bone micro-damage (micro-cracks) in case of cyclic load. In the guinea-pig experiments, an increase in δ BM between test and control peri-implant bone could be shown with increasing force amplitude (De Smet et al. 2006). From a generic finite element calculation of this guinea-pig implant model (Fig. 2c), it was estimated that a force amplitude of 6 N causes peri-implant bone strains in the order of magnitude of 2000–3000 μstrains next to the implant, which should be considered an osteogenic stimulus according to Frost's mechanostat (Frost 1987). From this simplified finite element, it is obvious that the highest strains are observed next to the implant surface (ROI 500 μm). Further away from the implant, the strain decreases, resulting in less pronounced δ BM.

It has been shown that bone responds especially to dynamic rather than static loads (Duyck et al. 2001, Robling et al. 2001). This means that cortical bone adaptation is not solely dependent on strain amplitude, but that cyclic loads have the potential to induce bone formation (Jagger et al. 1995). Mechanical stimulus parameters such as strain rate (Mosley & Lanyon 1998), frequency, number of loading cycles (Turner et al. 1994, Robling et al. 2002) and strain distribution and gradient (Judex et al. 1997), will all influence the cortical bone-adaptive response. Strain rate can further be decomposed into strain amplitude and loading frequency. A positive relationship between loading frequency and bone formation has been demonstrated in several studies (Rubin & McLeod 1984, Hsieh & Turner 2001).

In this model, although the same strain rate was applied, the effect of early mechanical stimulation decreased with decreasing force amplitude and increasing frequency. In the ulna axial compression model in mice, a dose–response relationship between loading frequency and cortical bone adaptation reaching a plateau with frequencies beyond 10 Hz has been shown (Warden & Turner 2004). The mechanism for this non-linear frequency response is not known, but the authors also confirmed, based on strain gauge measurements, that no dampening of the mechanical loading associated with high-frequency loading occurred. For the high-frequency group of the guinea-pig experiments, δ BM reaching a plateau could not be shown, but instead our results showed a lower effect of high-frequency mechanical stimulation than for the 3 Hz frequency stimulation protocol. Using the rat tibia four-point bending model, cortical bone responded to frequencies of 0.5 Hz and above, but not to lower frequencies (Turner et al. 1995). More recently, using the rat ulna axial loading model, it was found that cortical bone formation increased successively with increasing loading frequency up to 10 Hz (Hsieh & Turner 2001). Bone healing around a roughened implant was found to be improved by loading the functionally isolated turkey ulna at a frequency of 20 rather than 1 Hz (Rubin & McLeod 1984). These data seem to indicate that an increase in loading frequency results in an increase in an adaptive response of cortical bone.

However, the effects of frequency should not be isolated from the effects of the cycle number (Kaspar et al. 2002). At a constant frequency, the proliferate response of human bone-derived grown cells increased with the number of applied cycles until a maximum of 1800

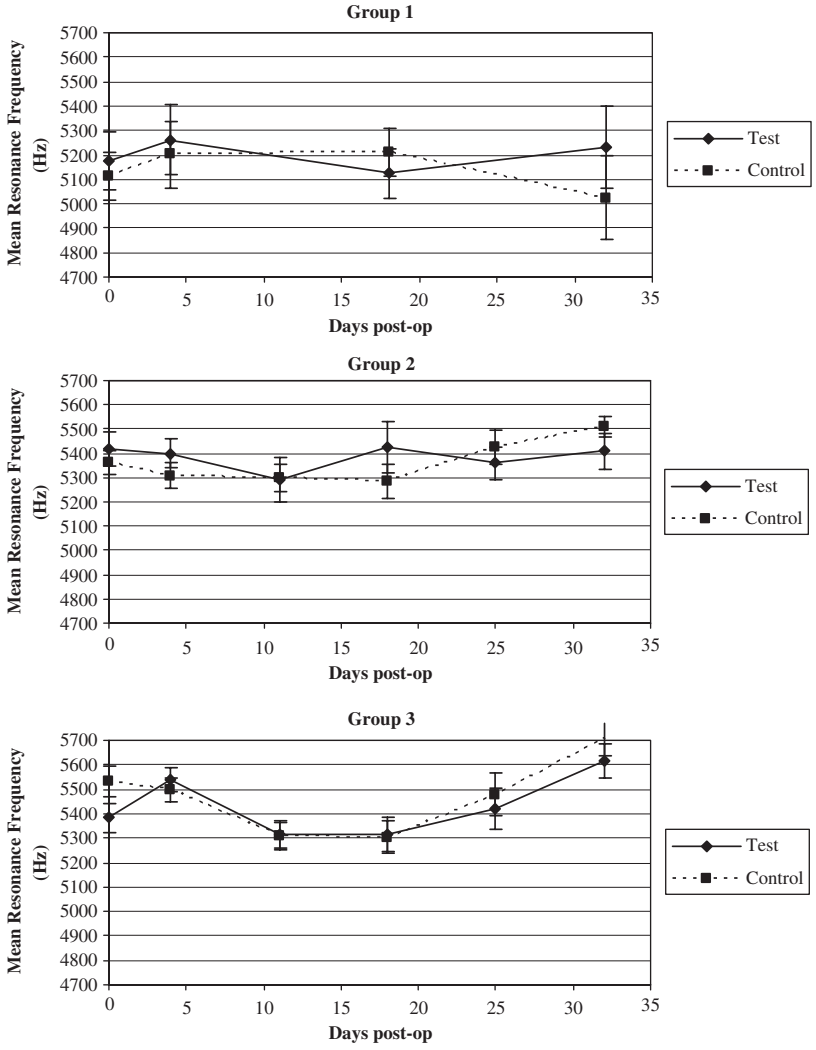

Fig. 5. Mean resonance frequencies (Hz) of test and control implants in the three groups. Stability analysis was performed at implant installation and from then on weekly (for series 1 every 2 weeks from the start of stimulation). Significant differences were found neither between test and control implants nor between the groups.

cycles was reached. Data suggest that the number of applied load cycles within a given time frame plays an important role in bone structural adaptation in vivo (Rubin & Lanyon 1984).

Recent research has shown trabecular bone to be responsive to very low-magnitude mechanical stimuli (0.3 g/5 μstrain) introduced at a high frequency (30 Hz) (Rubin et al. 2001, 2002). It is possible that the mechano-transductive pathways in cortical and trabecular bone differ and that the pathways respond differently to an equivalent mechanical stimulus. Nowadays, several reports suggest that osteocytes, which are terminally differentiated osteoblasts and that are present throughout the entire mineralized bone matrix, are the primary candidates for bone mechano-sensing (Weinbaum et al. 1994, Cowin et al. 1995, Burger & Klein-Nulend 1999). In particular, it is hypothesized that bone interstitial fluid flow through the canalicular network, which is induced by fluid pressure gradients in the deforming bone matrix, activates certain intra-cellular processes in the osteocytes. Biochemical signals, released by the osteocytes, would then in turn regulate osteoblastic and osteoclastic activity (Burger & Klein-Nulend 1999).

A significant positive effect of mechanical stimulation on bone-to-implant contact could not be shown in this study, although there was a trend for more bone-to-implant contact at the compressive (distal) *versus* tensile (proximal) side for the mechanically stimulated implants *versus* the controls. This is in agreement with data from another study with different implant geometry (De Smet et al. 2006). Moreover, hardly any change in implant stability measured by RF could be evidenced. This could be due to the bicortical fixation of the implants in the tibial bone, which was already high initially at implant installation. In a clinical study using RFA, Barewal et al. (2003) neither showed significant changes in implant stability during a 10-week period after implant installation for implants installed in Type I bone (Lekholm & Zarb 1985). However, a numerical simulation study and in vitro measurements for the guinea-pig experiments showed that the transducer orientation, the part of the bone around the implant and the boundary conditions (fixation of the tibia), influences the resonance frequency value measured by the Osstell system (Pattijn et al. 2007). In the guinea-pig model where the conditions deviate strongly from those in human dental practice, the Osstell technique does not allow the comparison of the stability between different implants due to poor repeatability and to the fact that the resonance frequency is determined by the whole bone–implant–transducer system and not only by the quality of the bone–implant interface (Pattijn et al. 2006).

This study explored a potential animal model showing that the in vivo force can be controlled experimentally to study quantitative biomechanical-mediated bone adaptation under various loading situations. Eventually, this may lead to a better understanding of improved early loading protocols of oral implants in humans. Differences in bone re-modelling rates between guinea-pig and humans can limit the extrapolation of the present data. Interpretation of animal data to humans needs to be carefully studied. Therefore, suggested principles of bone adaptation should be simulated first on individualized finite element models and validated to the results of the animal experiment before these can be considered for extrapolation to bone tissue application in humans.

While in these experiments the strain rate was kept unchanged, in a subsequent study the frequency will be kept constant. The latter will help us learn more about the importance of the force amplitude at low-frequency stimulation.

Conclusion

The present data show an optimization of the BM around controlled

early-loaded implants. The effect of early mechanical stimulation of peri-implant bone is strongly dependent on the strain/frequency and not on the strain rate as such for a constant period of stimulation. This cortical bone model has been shown to be most sensitive to low-frequency/high-amplitude stimulation.

Acknowledgements

S. Goovaerts and J. Vanhulst (Department of Biomechanics & Engineering Design; Metallurgy & Materials Engineering, KU Leuven) are acknowledged for technical support.

S. Cecere (Biostatistical Centre, School of Public Health, Leuven, Belgium) is acknowledged for the statistical analysis.

References

Barewal, R. M., Oates, T. W., Meredith, N. & Cochran, D. L. (2003) Resonance frequency measurements of implant stability in vivo on implants with a sandblasted and acid-etched surface. *International Journal of Oral and Maxillofacial Implants* **18**, 641–651.

Burger, E. H. & Klein-Nulend, J. (1999) Responses of bone cells to biomechanical forces *in vitro*. *Advances in Dental Research* **13**, 93–98.

Cowin, S. C., Weinbaum, S. & Zeng, Y. (1995) A case for bone canaliculi as the anatomical site of strain generated potentials. *Journal of Biomechanics* **28**, 1281–1297.

De Smet, E., Jaecques, S., Wevers, M., Jansen, J., Jacobs, R., Vander Sloten, J. & Naert, I. (2006) A guinea pig experimental study on the effect of controlled early mechanical implant loading on bone healing and bone mass: an *in vivo* micro-CT follow-up and histological study. *European Journal of Oral Sciences* **114**, 232–242.

Duyck, J., Ronold, H. J., Van Oosterwyck, H., Naert, I., Vander Sloten, J. & Ellingsen, J. E. (2001) The influence of static and dynamic loading on the marginal bone behaviour around implants: an animal experimental study. *Clinical Oral Implants Research* **12**, 207–218.

Frost, H. M. (1983) A determinant of bone architecture: the minimum effective strain. *Clinical Orthopaedics and Related Research* **175**, 286–292.

Frost, H. M. (1987) Bone 'mass' and the 'mechanostat': a proposal. *Anatomical Records* **219**, 1–9.

Frost, H. M. (1992) Perspectives: bone's mechanical usage windows. *Bone and Mineral* **19**, 257–271.

Hsieh, Y. F., Robling, A. G., Ambrosius, W.T., Burr, D. B. & Turner, C. H. (2001) Mechanical loading of diaphysial bone *in vivo*: the strain threshold for an osteogenic response varies with location. *Journal of Bone and Mineral Research* **16**, 2291–2297.

Hsieh, Y.F & Turner, C. H. (2001) Effects of loading frequency on mechanically induced bone formation. *Journal of Bone and Mineral Research* **16**, 918–924.

Jagger, C. J., Chambers, T. J. & Chow, J. W. (1995) Stimulation of bone formation by dynamic mechanical loading of rat caudal vertebrae is not suppressed by 3-amino-1-hydroxypropylidene-1-bisphosphonate (AHPrBP). *Bone* **16**, 309–313.

Judex, S., Gross, T. S. & Zemicke, R. F. (1997) Strain gradients correlate with sites of exercise-induced bone-forming surfaces in the adult's skeleton. *Journal of Bone and Mineral Research* **12**, 1737–1745.

Kaspar, D., Seidl, W., Neidlinger-Wilke, C., Beck, A., Claes, L. & Ignatius, A. (2002) Proliferation of human-derived osteoblast-like cells depends on the cycle number and frequency of uni-axial strain. *Journal of Biomechanics* **35**, 873–880.

Klein, C. P. A. T., Sauren, Y. M. H. F., Modderman, W. E. & Van der Waerden, J. P. C. M. (1994) A new saw technique improves preparation of bone sections for light and electron microscopy. *Journal of Applied Biomaterials* **5**, 369–373.

Lekholm, U. & Zarb, G. A. (1985) Patient selection and preparation. In: Brånemark, P.-I., Zarb, G. A. & Albrektsson, T., eds. *Tissue Integrated Prostheses – Osseointegration in Clinical Dentistry*. Chicago: Quintessence, 199–209.

Mosley, J. R. & Lanyon, L. E. (1998) Strain rate amplitude as a controlling influence on adaptive modelling in response to dynamic loading of the ulna in growing male rats. *Bone* **23**, 313–318.

Pattijn, V., Jaecques, S., De Smet, E., Muraru, L., Van Lierde, C., Van der Perre, G., Naert, I. & Vander Sloten, J (2007) Resonance frequency analysis of implants in the guinea pig model: influence of boundary conditions and orientation of the transducer. *Medical Engineering and Physics* **29**, 182–190.

Robling, A. G., Duijvelaar, K. M., Geevers, J. V., Ohashi, N. & Turner, C. H. (2001) Modulation of appositional and longitudinal bone growth the rat ulna by applied static and dynamic force. *Bone* **29**, 105–113.

Robling, A. G., Hinant, F. M., Burr, D. B. & Turner, C. H. (2002) Improved bone structure and strength after long-term mechanical loading is greatest if loading is separated into short bouts. *Journal of Bone and Mineral Research* **17**, 1545–1554.

Rubin, C. & Lanyon, L. (1984) Regulation of bone transformation by applied dynamic loads. *Journal of Bone and Joint Surgery* **66**, 397–402.

Rubin, C. T. & Lanyon, L. (1985) Regulation of bone mass by mechanical strain magnitude. *Calcified Tissue International* **37**, 411–417.

Rubin, C. T. & McLeod, K. J. (1984) Promotion of bony ingrowth by frequency-specific, low-amplitude mechanical strain. *Clinical Orthopaedics and Related Research* **298**, 165–174.

Rubin, C., Turner, A. S., Bain, S., Mallinckrodt, C. & McLeod, K. (2001) Low mechanical signals strengthen long bones. *Nature* **412**, 603–604.

Rubin, C., Turner, A. S., Mallinckrodt, C., Jerome, C., McLeod, K. & Bain, S. (2002) Mechanical strain, induced noninvasively in the high-frequency domain, is anabolic to cancellous bone, but not cortical bone. *Bone* **30**, 445–452.

Turner, C. H. (1998) Three rules for bone adaptation. *Bone* **23**, 399–407.

Turner, C. H., Forwoodm, M. R. & Otter, M. W. (1994) Mechanotransduction in bone: do bone cells act as sensors for fluid flow? *The Federation of American Societies for Experimental Biology Journal* **8**, 875–878.

Turner, C. H., Yoshikawa, T., Forwood, M. R., Sun, T. C. & Burr, D. B. (1995) High frequency components of bone strain in dogs measured during various activities. *Journal of Biomechanics* **28**, 39–44.

Van Der Lubbe, H. B. M., Klein, C. P. A. T. & De Groot, K. (1988) A simple method for preparing thin histological sections of undecalcified plastic embedded bone with implants. *Stain Technology* **63**, 171–177.

Warden, S. J. & Turner, C. H. (2004) Mechanotransduction in cortical bone is most efficient at loading frequencies of 5–10 Hz. *Bone* **34**, 261–270.

Weinbaum, S., Cowin, S. C. & Zeng, Y. (1994) A model for the excitation of osteocytes by mechanical loading induced bone fluid shear stresses. *Journal of Biomechanics* **27**, 339–360.

Address:
I. E. Naert
Department of Prosthetic Dentistry/BIOMAT Research Group
School of Dentistry
Oral Pathology and Maxillofacial Surgery
Faculty of Medicine
K. U. Leuven
Kapucijnenvoer 7, 3000 Leuven
Belgium
E-mail: Ignace.Naert@med.kuleuven.be

Clinical Relevance

Scientific rationale: Today, there is a shift towards faster implant loading. Local loading is believed to be strongly determine the processes of bone formation/resorption around implants.

Principal findings: This animal study shows that early loading does not impair implant healing and that strain rate is not the determining parameter. Early mechanical stimulation, with an optimal low frequency (3 Hz)/high amplitude (2 N), increases peri-implant bone mass.

Practical implications: Differences in re-modelling rates between animals and humans need careful interpretation. Once the influence of mechanical parameters is understood, a general model for adaptive bone re-modelling can be applied to the human jawbone.